Effects of Surfactants on the Phase Transition of Poly(*N*-isopropylacrylamide) in Water

CHI WU* and SHUIQIN ZHOU

Department of Chemistry, The Chinese University of Hong Kong Shatin, N.T., Hong Kong

SYNOPSIS

The effects of both anionic (sodium dodecyl sulfate, SDS) and cationic (dodecylpyridine bromide, DPB) surfactants on the phase transition of narrowly distributed poly(*N*-isopropylacrylamide) (PNIPAM) microgel particles were investigated by laser light scattering. The addition of SDS swells the particles and increases the phase transition temperature, while DPB has a much smaller effect. This difference cannot be due to an association between the surfactant hydrophobic tail and PNIPAM because DPB and SDS have an identical hydrophobic tail. The amide groups in PNIPAM are slightly protonized in deionized water (pH ~ 5.5). Our results contradict a previous prediction that oppositely charged surfactants will collapse a polyelectrolyte gel. After adding SDS, a two-step phase transition of the PNIPAM gel is observed. This suggests that SDS forms micelles inside the microgel with the help of the immobilized counter ions on the gel network. The SDS micelles are broken into individual SDS molecules in the first step of phase transition, while in the second step individual SDS molecules are gradually expelled. Surfactant effects on the microgel particles are compared with those of individual PNIPAM chains. © 1996 John Wiley & Sons, Inc.

Keywords: Poly(*N*-isopropylacrylamide) • phase transition • surfactant effects • laser light scattering

INTRODUCTION

The phase transition and critical phenomena in polymer gels, especially in various kinds of polyelectrolytes gels, have been extensively studied in the last decade.[1] It has been discovered that a certain type of gel made of either synthetic or natural polymers can undergo volume-phase transitions in response to a small change in its environment, such as temperature, light, ion strength, pH, and electric field.[2-6] These gels are labelled as intelligent gels. The volume-phase transitions are sometimes reversible and discontinuous, which leads to some speculated applications, such as temperature sensor, controlled drug-releasing devices, artificial muscle, and polymer transducers.[7]

On the basis of the Flory theory[8] for the swelling/shrinking of polymer networks, Dusek and Patterson[9] proposed a theory for the volume phase transition. Later, the theory was modified by Tanaka for the discrete volume phase transition of some partially ionized polyacrylamide gels.[10] It is known that the swelling/shrinking of a polymer network is closely linked to the phase transition of a single chain from an extended coil in a good solvent to a collapsed globule in a poor solvent.[11,12] Theoretical and experimental studies of the coil-to-globule transition of a single chain have been extensively conducted.[13-16] Recently, we have studied the volume phase transition of poly(*N*-isopropyl-acrylamide) (PNIPAM) in water.[17] We started with the coil-to-globule transition of a single well-defined high-molecular weight PNIPAM chain; then the volume phase transition of the PNIPAM microgel particles; and finally, the swelling/shrinking of ultra-thin PNIPAM gel films. A comparison of individual chains with the microgel particles leads to a better understanding of the volume phase transition of bulk PNIPAM gels.

The influence of surfactants on the PNIPAM volume phase transition has been actively studied.[18-24] Most studies were with the interaction of

* To whom correspondence should be addressed.

Journal of Polymer Science: Part B: Polymer Physics, Vol. 34, 1597–1604 (1996)
 CCC 0887-6266/96/091597-08

surfactants with modified PNIPAM linear chains. Generally, surfactant promotes both inter- and intramolecular solubility so that the phase transition temperature (T_c) increases with the surfactant concentration. An association of the surfactant hydrophobic tails with the hydrophobic side groups or backbone of PNIPAM has been suggested to answer for these results. Recently, Khokhlov et al.[25] predicted that the interaction of a polyelectrolyte gel with an oppositely charged surfactant presents three effects: At low concentration, the surfactant cannot form micelles inside the network and the gel behaves as in the solution of low molecular-weight salts so as to shrink slightly. At higher concentration, the surfactant molecules inside the gel exceed the critical micelle concentration (CMC) so that micelles are formed and the gel collapses because of a decrease of the osmotic pressure exerted by the surfactant. At still higher surfactant concentration, no additional micelles are formed inside the network and the network dimensions coincide with those of the neutral network. However, the results from different laboratories are contradictory and both discontinuous and continuous volume phase transitions have been observed for a similar PNIPAM/water system. Here, we study the effects of cationic and anionic surfactants with narrowly distributed PNIPAM microgel particles. The volume phase transition of the microgel particles is compared with the coil-to-globule transition of single PNIPAM chains.

EXPERIMENTAL

Sample Preparation

N-isopropylacrylamide (NIPAM) (Eastman Kodak) was recrystallized three times in a benzene/*n*-hexane mixture. *N,N'*-methylenebis-(acrylamide) (BIS) as a crosslinker was recrystallized from methanol. Potassium persulfate (KPS) (from Aldrich, analytical grade) as an initiator and anionic surfactant sodium dodecyl sulfate (SDS) (BDH, 99%) as dispersant were used without further purification. First, 240 mL dust-free deionized water, 3.84 g NIPAM, 0.0730 g BIS, and 0.0629 g SDS were added to a 500 mL reactor fitted with a glass stirring rod, a Teflon paddle, a reflux condenser, and a nitrogen bubbling tube; then, the solution was heated to 70°C and stirred at 200 rpm for 40 min with a nitrogen purge to remove oxygen; finally, 0.1536 g KPS dissolved in 25 mL dust-free deionized water was added to start the polymerization. The reaction mixture was stirred for 4.5 h. The microgel particles were purified and diluted to ca. 10^{-6} g/mL for LLS measurements. Trace amounts of SDS remained in the final dilute solution. It has been proven that if the SDS concentration is lower than 3×10^{-4} g/mL, SDS has no effect on the phase transition of PNIPAM in water.[26] Hereafter, we will refer to this original dilute solution as surfactant-free or $C_{SDS} \sim 0.0$ g/mL in contrast to other solutions wherein surfactants are added. Dodecylpyridine bromide (DPB, from Beijing University, China) was used as a cationic surfactant. The resistivity of the deionized water used here was 18.3 MΩ · cm and pH = ca. 5.5. Detail of the preparation of the PNIPAM microgel particles can be found elsewhere.[20]

Laser Light Scattering (LLS)

In static LLS, the excess time-averaged scattered light (ΔI) intensity over water was measured. According to the LLS theory for a dilute solution at a small scattering angle θ,[27,28] the weight-average molecular weight M_w can be related to ΔI as

$$\Delta I \propto \mathrm{KCM}_w P(q)/[1 + 2A_2 M_w P(q)C] \qquad (1)$$

with $P(q) \cong 1 - (1/3)R_g^2 q^2$, *where* $K = 4\pi^2 n^2 \left(\frac{dn}{dC}\right)^2/(N_A \lambda_o^4)$ with N_A, n and λ_o being Avogadro's number, the solvent refractive index, and the wavelength of light, respectively; $q = (4\pi n/\lambda_o)\sin(\theta/2)$; R_g is the average radius of gyration; C is polymer or particle concentration; and A_2 is the second virial coefficient. When C is very low ($\sim 10^{-6}$ g/mL), the term $2A_2 M_w P(q)C$ can be dropped out. At $q \to 0$, ΔI is only related to dn/dC and M_w for a given polymer/solvent system.

In dynamic LLS, $G^{(2)}(t, q)$, the intensity-intensity time correlation function was measured in the self-beating mode. It can be related to $g^{(1)}(t, q)$, the normalized electric field time correlation function, by[29,30]

$$G^{(2)}(t, q) = A[1 + \beta |g^{(1)}(t, q)|^2] \qquad (2)$$

where A is a measured baseline; β, a parameter depending on the coherence of the detection; and t, the delay time. $g^{(1)}(t, q)$ is related to the line-width distribution $G(\Gamma)$ by

$$g^{(1)}(t, q) = \int_o^\infty G(\Gamma) e^{-\Gamma t} d\Gamma \qquad (3)$$

where the line-width Γ is usually a function of both C and θ.[31] $G(\Gamma)$ can be calculated from the Laplace inversion of $G^{(2)}(t, q)$ on the basis of eqs. (2) and (3). If the relaxation is diffusive, Γ is related to the diffusion coefficient D by $\Gamma/q^2 = D$ when $C \to 0$ and $q \to 0$. In this case, $G(\Gamma)$ can be directly converted to a diffusion coefficient distribution $G(D)$ or a hydrodynamic radius distribution $f(R_h)$ by using the Stokes-Einstein equation, $R_h = k_B T/(6\pi\eta D)$ where k_B is the Boltzmann constant.

A commercial LLS spectrometer (ALV/SP-150 equipped with an ALV-5000 digital time correlator) was used with a solid-state laser (ADLAS DPY425II, output power ca. 400 mW at λ = 532 nm) as the light source. The incident laser light beam was vertically polarized with respect to the scattering plane and the light intensity was regulated with a beam attenuator (Newport M-925B) so as to avoid a possible localized heating in the scattering cuvette. In our setup, the coherent factor β in dynamic LLS is ca. 0.87, a rather high value for a spectrometer capable of doing both static and dynamic LLS simultaneously. With some proper modifications,[32] our LLS spectrometer is capable of doing both static and dynamic LLS continuously in the wide range of 6–154°. The accessible small-angle range is particularly useful in the measurement of larger size microgel particles since the condition of $R_g q < 1$ is required in static LLS to precisely determine M_w and R_g. The long-term temperature stability inside our LLS sample holder was $\sim \pm 0.02$°C.

RESULTS AND DISCUSSION

Figure 1 shows the SDS concentration dependence of $f(R_h)$ of the PNIPAM microgel particles at T = 22°C. The microgel particles are narrowly distributed with an initial average hydrodynamic radius of ca. 180 nm and swell as C_{SDS} increases. When C_{SDS} is higher than 2.6 mM, the radius of the microgel particle has reached its limit value of ca. 250 nm and the maximum relative increase in radius is ca. 40%. Meewes et al.[26] showed that for individual PNIPAM linear chain in water, the chain expansion stopped when $C_{SDS} \geq$ ca. 2.4 mM and the maximum relative increase is only ca. 20%. Both of the particle swelling and chain expansion cease before C_{SDS} reaches the critical micelle concentration (CMC, 9.0 mM) of SDS in pure water at 22°C. The difference in the relative size increase does not mean that the short subchain inside the PNIPAM microgel particles can expand easier than the long PNIPAM linear chain free in water. Instead, this difference is

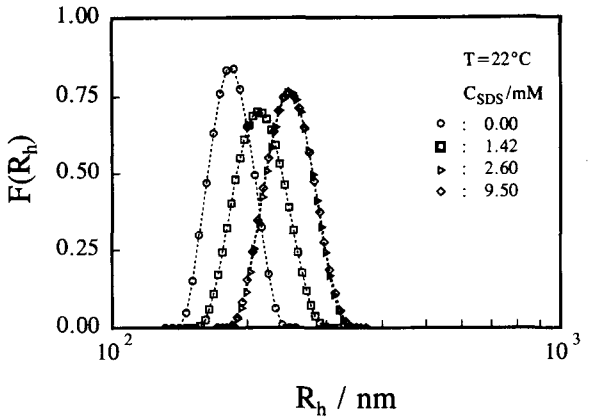

Figure 1. SDS concentration dependence of the hydrodynamic radius distribution $f(R_h)$ of the PNIPAM microgel particles at 22°C.

attributed to the initial chain dimension difference between the free chain and subchain inside the gel network. Our results and the results in ref. 26 indicate that there is no difference in the solvent quality for the particles and linear PNIPAM chains as long as C_{SDS} > ca. 2.4 mM, i.e., the PNIPAM chain has reached its stretching limit.

By using $\rho = M_w/[(\frac{4}{3})\pi R_h^3]$, we estimated the chain segment density ρ for both the linear chains and microgel particles at different C_{SDS} with the values of M_w and R_h. For the linear PNIPAM chains in water at 25°C, $\rho = 2.8 \times 10^{-3}$ g/cm^3 at $C_{SDS} = 0$ and $\rho = 1.6 \times 10^{-3}$ g/cm^3 at $C_{SDS} \sim$ 2.4 mM; and for the PNIPAM microgel particles in water at room temperature, $\rho = 1.7 \times 10^{-2}$ g/cm^3 at $C_{SDS} = 0$ and $\rho = 6.0 \times 10^{-3}$ g/cm^3 at C_{SDS} ca. 2.6 mM. The chain segment density of the microgel particles is higher than that of free PNIPAM linear chains in water even at its expansion limit because the crosslinking inside the microgel particles.

Figure 2 shows the hydrodynamic radius distribution $f(R_h)$ of the PNIPAM microgel particles at three DPB concentrations, where T = 22°C. It is known that DPB has a very similar CMC as SDS in water at 22°C. Figure 2 clearly shows that the addition of DPB has very little effect on the size of the microgel particles at 22°C. It is worth noting that SDS and DPB have an identical hydrophobic tail, $CH_3(CH_2)_{11}^-$. The only difference between SDS and DPB is their small hydrophilic head, i.e., $-SO_4^-$ (anionic) for SDS and $-N^+(CH)_5$ (cationic) for DPB.

According to the interaction/association model proposed in Figure 6 of ref. 20, the hydrophobic tail of SDS is adsorbed on the hydrophobic backbond of PNIPAM to form spherical micelles (like a series

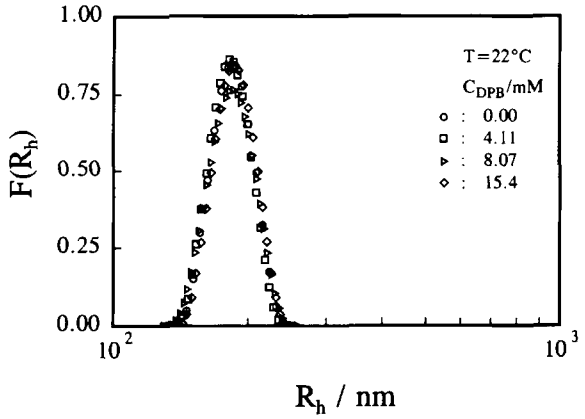

Figure 2. DPB concentration dependence of the hydrodynamic radius distribution $f(R_h)$ of the PNIPAM microgel particles at 22°C.

of beads connected by PNIPAM) or cylindrical micelles (like a series of sausages connected by PNIPAM). This contradicts our observation, because if correct, i.e., the swelling of the PNIPAM microgel particles would depend only on the nature of the hydrophobic tail, such as its length and structure, we would observe a similar surfactant effect for SDS and DPB. This clear discrepancy forced us to search for another model to explain the different surfactant effects observed for SDS and DPB. First, we noted that the nitrogen of the amide group has one pair of electrons (i.e., electron-rich). Second, Schild and Tirrell[18] have reported that with the assistance of a very small amount of PNIPAM (ca. 1.5 mM) surfactant SDS can form micelles at a concentration 10-fold lower than the CMC of SDS in pure water. Their results lead to a general picture of the PNIPAM-assisted SDS micelle formation.

Figure 3 shows a schematic of the interaction and association between SDS and the PNIPAM microgel network. From the initial composition, we know that on average the subchain between two neighbor crosslinking points has ca. 100 NIPAM monomer units with a stretched length of ca. 25 nm. The microgel network can be viewed as a three-dimensional regular cubic lattice made of a very long PNIPAM chain. We can calculate the total length (L) of the chain from the particle mass M_w ($\sim 2.2 \times 10^8$ g/mol); and the number (N) of the subchains from the average particle radius $\langle R_h \rangle$ (ca. 250 nm and ca. 65 nm, respectively, for the swollen and collapsed particles) and the actual average subchain length (l) by using a simple geometrical consideration. As the only unknown parameter, l can be estimated from $L = Nl$. The estimates of l are ca. 25 and ca. 6 nm for the microgel particles at the swelling and collapsing limits, respectively. At the swelling limit, l is very close to the stretched length of the subchains, which shows that the network is highly extended. This is why further addition of SDS after C_{SDS} > ca. 2.4 mM has no effect on the swelling as shown in Figure 1.

In this model, the concentration of SDS molecules inside the gel network is much higher than that outside the gel network because the hydrophobic attraction. It is expected that there exists a repulsion between SDS molecules and the electron-rich amide group on the gel network. Therefore, SDS molecules might be able to form micelles (ca. 4–5 nm in diameter) inside the gel network, even though the

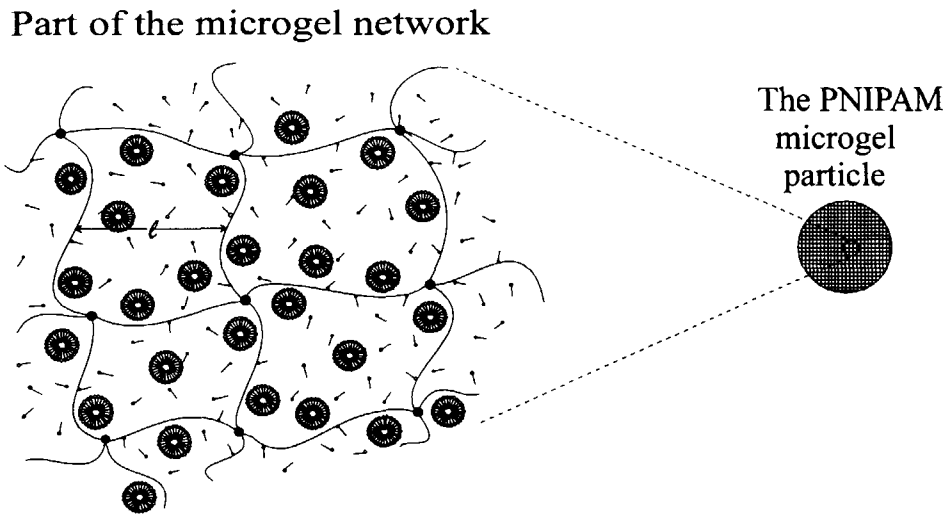

Figure 3. Schematic of the interaction/association between SDS and the microgel network inside the PNIPAM particles.

overall concentration of SDS is lower than its CMC in pure water. Such formed micelles are loosely confined inside the PNIPAM gel. The model in Figure 3 looks very similar to the one in Figure 1 of ref. 25. However, there is a difference between these two models, namely the model in Figure 3 has considered the repulsion between micelles and between micelles and the network, which lead to the extension of the subchains and the swelling of the gel network.

This is similar to polyelectrolytes in water with extended chain conformation because of the repulsion between the ionized groups along the backbond chain. The only difference here is that the steric hinderance of large micelles makes the chain more rigid and extended. As C_{SDS} increases, more SDS micelles are formed inside the network so that the particle swells further. However, the number of the micelles able to exist inside the microgel network is limited. When that limit is reached, the swelling ceases. Experimentally, we found this limit to be ca. 2.4 mM for SDS in the PNIPAM microgel network. As shown in Figure 3, the model does not exclude the existence of individual SDS molecules free inside the gel network.

In contrast, cationic DPB molecules can be attracted to the amide group. On one hand, this attraction reduces the hydrophilicity of the PNIPAM microgel network; and on the other hand, this might prevent the formation of micelles inside the gel network. This is why the addition of DPB has less effect on the swelling of the microgel particles. Actually, in this case, water becomes a poor solvent for the microgel network. Later, we will show that the addition of DPB can lead to the shrinking of the microgel network at room temperature and aggregation of the microgel particles at high temperature. The model presented in Figure 3 is further examined in the following phase transition experiments.

Figure 4 shows the temperature-dependence hydrodynamic radius distribution $f(R_h)$ of the microgel particles. The particles are swollen at $T = 30.2$°C and collapsed at $T = 57$°C. The average hydrodynamic radius $\langle R_h \rangle$ decreases four times, which means a ca. 60-time change in the PNIPAM chain segment density, i.e., from ca. 6.0×10^{-3} g/cm^3 to $\sim 3.2 \times 10^{-1}$ g/cm^3. By assuming the density of the microgel particle (includes the PNIPAM microgel network and the water molecules encapsulated inside) to be ~ 1 g/cm^3, we can estimate that each microgel particle contains more than 99% of water in the swollen state and ca. 70% of water in the collapsed state. As expected, Figure 4 shows that the shape and width of $f(R_h)$ remained during the phase transition because the swelling and collapsing occurred within each particle.

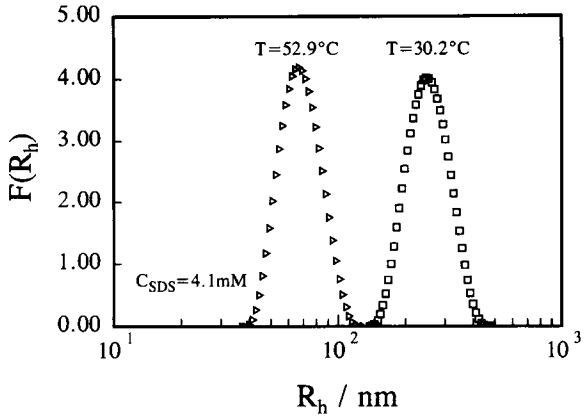

Figure 4. Temperature dependence of the hydrodynamic radius distribution $f(R_h)$ of the PNIPAM microgel particles.

Figure 5 shows the hydrodynamic radius distribution $f(R_h)$ of the PNIPAM microgel particles at the collapsing limit ($T > T_c$). In comparison with Figure 1, the amount of added SDS has little effect on the collapsed particles. On the basis of the model shown in Figure 3, this discrepancy is expected. When water is a good solvent at $T = 22$°C as in Figure 1, the PNIPAM microgel network swells in water and SDS molecules can enter the network to form micelles inside, which further swells the particles until the subchains are fully stretched, whereas when $T > T_c$ water becomes a poor solvent, so that the particles collapse and water molecules together with surfactant molecules are expelled from the gel network. The fact that $f(R_h)$ is independent on C_{SDS} strongly indicates that at the collapsing limit most surfactant molecules are outside of the gel network. The estimate value of l at the collapsing limit indicates that it would be difficult to confine the SDS micelle inside such small mesh holes.

Figure 6 shows the influence of surfactant SDS on the phase transition of the microgel particles. When $C_{SDS} = 9.5$ mM, the swollen particles are so stable that T_c was shifted to a much higher temperature beyond our LLS instrument limit. Besides the increase of T_c, there are two remarkable features of the phase transition in Figure 6. First, with or without adding SDS, the phase transition is continuous, which agrees with the results observed for both individual PNIPAM chains and macroscopic gels,[18,19,21-23] but contradicts the reported discontinuous volume phase transition.[20] It is known that the polymer chains with different lengths will undergo the phase transition at different temperatures. Be-

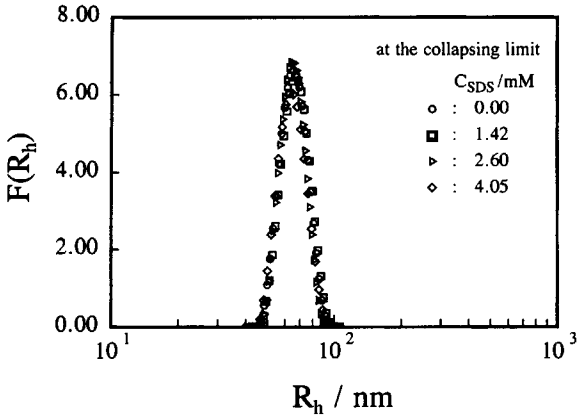

Figure 5. Hydrodynamic radius distribution $f(R_h)$ of the PNIPAM microgel particles at the collapsing limit ($T > T_c$).

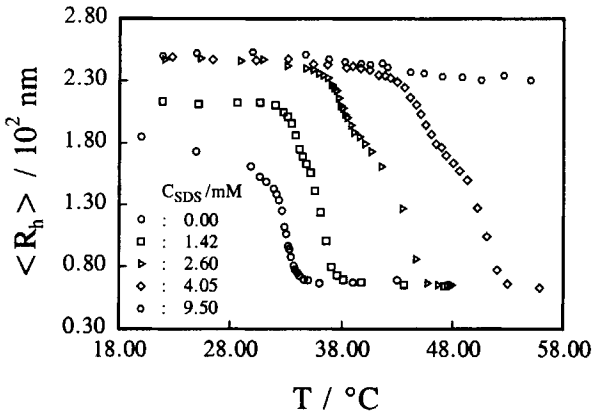

Figure 6. Influence of surfactant SDS on the phase transition of the microgel particles, where $\langle R_h \rangle$ [$= \int_o^\infty f(R_h)R_h dR_h$] is the average hydrodynamic radius.

cause of different subchain lengths, it is expected that the phase transition of a polymer gel be continuous. The discontinuous volume change observed for bulk PNIPAM gels can be attributed to the shear module, namely the shear module keeps the shape of a bulk gel until its internal stress builds to a certain point that the shear module can no longer maintain the shape of the gel and the gel will undergo an apparent discontinuous volume phase transition. On the other hand, it is known that it takes a very long time for a bulk gel to reach its true swelling and shrinking equilibriums.[33]

Second, when SDS is added the phase transition becomes sharp and undergoes a two-step transition which becomes more obvious as C_{SDS} increases. To our knowledge, this kind of two-step phase transition has been observed for the first time. In addition, our data showed that even without the addition of SDS the microgel particles are thermodynamically stable at the collapsing limit. There was no aggregation (phase separation) observed in the solution after more than one week. This is quite different from the collapsed single PNIPAM chain which is only kinetically stable (i.e., stable within a finite time period) ($\sim 10^3$ s). When $T > T_c$, the microgel particles shrink into individual collapsed spheres (still encapsulate ca. 70% of water in their hydrodynamic volume), but the interparticle attraction has been somehow prevented. Our speculation is that the anionic residual generated from the initiator might play an important role in this aspect. Another possibility is that during the phase transition the amide groups near the particle surface have a tendency to stay outside and form a hydrophilic surface layer which leads to the solubility of the particle as a whole.

Figure 7 shows the translational diffusion distribution $G(D)$ of the microgel particles at different temperatures during the phase transition. As T increases, the microgel particles undergo the phase transition and the particles collapse so that $G(D)$ shifts to the direction of higher D due to smaller hydrodynamic radius. It is interesting to note that before the collapse of the particles reaches the second step ($T < 45$°C), $G(D)$ has only a single narrow peak, whereas after entering the second step ($T > 45$°C), we start to see the appearance of another very small peak (it is enlarged in the logarithmic scale) located at a much higher D, i.e., some very small species in comparison with the microgel particles. The area ratio of the small peak to the large one increases and the position of the small peak essentially remains. We were astonished by this small peak and later we realized that this small peak can be related to the SDS micelles.

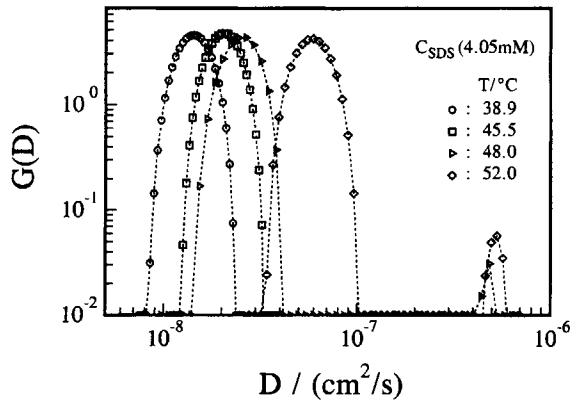

Figure 7. Temperature dependence of diffusion distribution $G(D)$ of the microgel particles during the phase transition.

Figure 7 leads us to the following explanations for the two-step collapsing shown in Figure 6. In the first step, the SDS micelles were broken as the particles collapsed, wherein the collapse of the particles and the break up of the micelles promote each other leading to a fast decrease of $\langle R_h \rangle$ as shown in Figure 6 (the first step). After the SDS micelles are broken and SDS molecules are expelled, the gel network will behave as one without the addition of SDS. It can be seen that in Figure 6 at the turning point between the first and second steps the particles have a similar size as those without adding SDS. Therefore, the second step corresponds to the shrinking of the gel without the presence of SDS. The SDS excluded from the gel particles are expected to be near the particle surface and form surfactant aggregates because of the hydrophobic attraction. The small $G(D)$ peak in Figure 7 might represent these surfactant aggregates.

Figure 8 shows two hydrodynamic radius distributions $f(R_h)$ of the microgel particles at the collapsing limit in the presence of SDS and DPB, respectively. It is clearly shown that the nature of the surfactant molecules has no effect on the microgel particles when the particles are in the collapsed state. This agrees with our above discussion, namely in the collapsed state surfactant molecules are expelled out. Figure 8 further shows that in the collapsing process surfactant molecules have been driven out. However, we cannot exclude the possibility that there might still exist a trace amount of surfactant molecules inside the gel network. If such is the case, this trace amount of surfactant molecules inside the network actually has no effect on the collapsed particles.

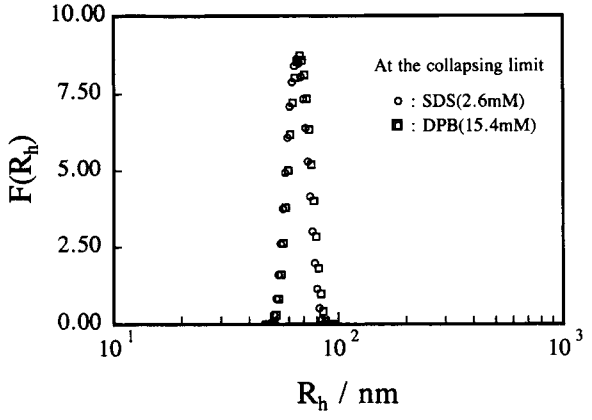

Figure 8. Influence of SDS and DPB on the hydrodynamic radius distribution $f(R_h)$ of the PNIPAM microgel particles at the collapsing limit.

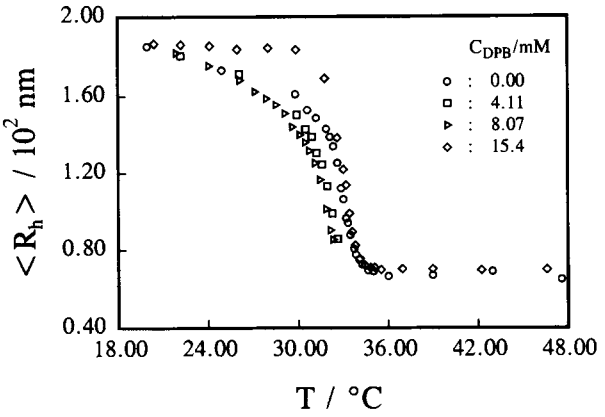

Figure 9. Influence of DPB on the phase transition of the PNIPAM microgel particles, where $\langle R_h \rangle$ is defined in Figure 6.

Figure 9 shows the influence of surfactant DPB on the phase transition of the microgel particles, where $\langle R_h \rangle$ is the average hydrodynamic radius of the particles. As we discussed before, cationic DPB molecules are attracted to the amide group to reduce the hydrophilicity of the gel network. This is why when C_{DPB} is lower than its CMC (ca. 12 mM) in pure water the phase transition temperature is slightly lower than that of the surfactant-free particles and the collapsed particles are unstable and $\langle R_h \rangle$ cannot reach the plateau in Figure 9 when C_{DPB} is 4.11 mM and 8.07 mM. When C_{DPB} is higher than the CMC, DPB will form micelles inside and outside the gel network, which swells the gel networks, increases the volume phase transition temperature, and stabilizes the gel particles even in the collapsing limit.

CONCLUSION

The study of phase transition of poly(*N*-isopropylacrylamide) (PNIPAM) microgel particles in the presence of anionic (sodium dodecyl sulfate, SDS) and cationic (dodecylpyridine bromide, DPB) surfactants enables us to propose a qualitative model for the micelle formation inside the microgel network. Our results showed that SDS molecules can form micelles inside the network. The repulsion between the micelles and the gel network extend the network. There exist two distinct steps in the volume phase transition. The first step involves the breaking up of the micelles and expelling of SDS from the gel network, while the second step represents the collapse of the surfactant-free gel network. On the other hand, cationic surfactant (DPB) is attracted

to the amide group and reduce the hydrophilicity of the gel network. This leads the shrinking of the particles and shifts the phase transition to a slightly lower temperature. However, if the DPB concentration is higher than the CMC, micelles will form inside and outside the gel network, so that the DPB micelles formed inside the gel network swell the particles and shift the phase transition temperature higher. The studies on the particles and single PNIPAM chains show that the phase transition of PNIPAM is continuous. In the collapsing limit, the density of the PNIPAM microgel network and individual linear chains are very similar.

We would like to thank Professor A. R. Khokhlov for his valuable comments about the manuscript and interpretation of our results. The financial support of the RGC (the Research Grants Council of Hong Kong Government) Earmarked Grant 1994/95 (CUHK 299/94P, 221600260) is gratefully acknowledged.

REFERENCES AND NOTES

1. K. Dusek, ed. *Adv. Polym. Sci.*, **109,** 110 (1993).
2. M. Shibayama, M. Morimoto, and S. Nomura, *Macromolecules,* **27,** 5060 (1994); and references therein.
3. A. Mamada, T. Tanaka, D. Kungwatchakum, and M. Irie, *Macromolecules,* **24,** 1605 (1990) and references therein.
4. M. Ilavsky, H. W. Ulmer, K. Nijenhuis, and W. J. Mijs, *J. Non-Crystalline Solids,* **172–174,** 935 (1994).
5. H. G. Schild, *Prog. Polym. Sci.*, **17,** 163 (1992).
6. T. C. Park and A. S. Hoffman, *Macromolecules,* **52,** 85 (1994).
7. Y. Osada and S. B. Ross-Murphy, *Sci. Am.*, **May,** 42 (1993).
8. P. J. Flory and J. Rehner, *Principles of Polymer Chemistry,* Cornell University Press, Ithaca, NY, 1953.
9. K. Dusek and D. Patterson, *J. Polym. Sci.*, **6,** 1209 (1968).
10. T. Tanaka, *Phys. Rev. Lett.*, **40,** 820 (1978).
11. W. H. Stockmayer, *Makromol. Chem.*, **35,** 54 (1960).
12. H. Yamakawa, *Modern Theory of Polymer Solutions,* Harper & Row, New York, 1971.
13. H. Yamakawa, *Macromolecules,* **26,** 5061 (1993).
14. B. Chu, I. H. Park, Q. W. Wang, and C. Wu, *Macromolecules,* **20,** 2883 (1987).
15. A. Y. Grosberg and D. V. Kuznetsov, *Macromolecules,* **26,** 4249 (1993) and references therein.
16. B. Chu, Q. C. Ying, and A. Y. Grosberg, *Macromolecules,* **28,** 180 (1995).
17. C. Wu and S. Q. Zhou, *Macromolecules,* (1995).
18. H. G. Schild and D. A. Tirrell, *Langmuir,* **7,** 665 (1991).
19. F. M. Winnik, H. Ringsdorf, and J. Venzmer, *Langmuir,* **7,** 912 (1991).
20. E. Kokufuta, Y. Q. Zhang, T. Tanaka, and A. Mamada, *Macromolecules,* **26,** 1053 (1993).
21. K. Tam, S. Ragaram, and R. Pelton, *Langmuir,* **10,** 418 (1994).
22. H. Yu and D. W. Grainger, *Macromolecules,* **27,** 4554 (1994).
23. T. G. Park and A. S. Hoffman, *J. Appl. Polym. Sci.*, **52,** 85 (1994).
24. K. Kubota, S. Fujishige, and I. Ando, *J. Phys. Chem.*, **94,** 5154 (1990).
25. A. R. Khokhlov, E. Y. Kramarenko, and E. E. Makhaeva, *Makromol. Chem., Theory Simul.*, **1,** 105 (1992).
26. M. Meewes, J. Ricka, M. Silva, R. Nyffenegger, and T. Binkert, *Macromolecules,* **24,** 5811 (1991).
27. B. H. Zimm, *J. Chem. Phys.*, **16,** 1099 (1948).
28. P. Debye, *J. Phys. & Coll. Chem.*, **51,** 18 (1947).
29. R. Pecora, *Dynamic Light Scattering,* Plenum Press, New York, 1976.
30. B. Chu, *Laser Light Scattering,* 2nd ed., Academic Press, New York, 1991.
31. W. H. Stockmayer and M. Schmidt, *Pure Appl. Chem.*, **54,** 407 (1982); *Macromolecules,* **17,** 509 (1984).
32. C. Wu, K. Chan, and K. Q. Xia, *Macromolecules,* **28,** 1032 (1995).
33. C. Wu and C. Y. Yan, *Macromolecules,* **27,** 4516 (1994).

Received June 29, 1995
Revised January 19, 1996
Accepted January 24, 1996